ELSEVIER

Thermochimica Acta 396 (2003) 43–56

thermochimica acta

www.elsevier.com/locate/tca

Temperature-modulated calorimetry of hexacontane and oligomer fractions of poly(oxyethylene) and poly(oxytetramethylene)☆,☆☆

Jeongihm Pak[a,*], Marek Pyda[b], Bernhard Wunderlich

[a] *Department of Chemistry, The University of Tennessee, Knoxville, TN 37996-1600, USA*
[b] *Chemical and Analytical Sciences Division, Oak Ridge National Laboratory, Oak Ridge, TN 37831-6197, USA*

Received 19 November 2001; received in revised form 18 July 2002; accepted 2 October 2002

Abstract

The paraffin hexacontane, $C_{60}H_{122}$, and oligomeric fractions of poly(oxyethylene), POE, and poly(oxytetramethylene), POTM, of varying low molar masses were studied with temperature-modulated calorimetry. The analyses were by standard differential scanning calorimetry (DSC) and quasi-isothermal, temperature-modulated DSC, TMDSC. Small sample masses were examined with temperature amplitudes from 0.05 to 2.5 K, using periods of 60 s. The supercooling decreases with molar mass for all three types of samples. The melting varied between fully irreversible, reversing, and largely reversible. There are no major differences in supercooling between extended- and folded-chain crystals. Due to conformational contributions, all crystals increase their heat capacities within the melting range from the level set by the vibrational spectrum to that of the liquid.
Published by Elsevier Science B.V.

Keywords: Supercooling; Melting; Crystallization; Quasi-isothermal TMDSC; Oligo(oxyethylene); Oligo(oxytetramethylene); Paraffin; Hexacontane; Polyethylene; DSC

1. Introduction

It is well known that crystallization usually does not occur at the equilibrium melting temperature, but needs a certain amount of supercooling. To initiate crystallization, at least primary nucleation is necessary in most cases since a free-enthalpy barrier hinders the formation of small crystals. This supercooling due to primary nucleation can be avoided by self-nucleation (nucleation by remaining or added crystals of the same type) or heterogeneous nucleation (nucleation by addition of foreign particles). For polymer molecules, however, primary nucleation is insufficient to overcome all free-enthalpy barriers, there is always a supercooling needed to crystallize, even in the presence of pre-existing crystals or nuclei [1,2]. A long, flexible molecule is not a small particle that can add directly in one step to a growing crystal, but appears in the melt or solution as a random coil and must first be extended to a certain degree before it can add sequentially to a pre-existing crystal surface. Typically, growing polymers possess lateral growth

☆ Presented in part at the 29th NATAS Conference in St. Louis, MO, 24–26 September 2001.

☆☆ The submitted manuscript has been authored by a contractor of the US Government under the contract No. DOE-AC05-00OR-22725. Accordingly, the US Government retains a non-exclusive, royalty-free license to publish, or reproduce the published form of this contribution, or allow others to do so, for US Government purposes.

* Corresponding author.
E-mail address: wunderlich@charterTN.net (J. Pak).

0040-6031/02/$ – see front matter. Published by Elsevier Science B.V.
PII: S0040-6031(02)00515-4

faces of extended chain segments of 5–50 nm lengths for continued crystallization, and surfaces across the chain direction which are inactive for further crystallization. A lamellar morphology is the common result of such crystallization. The need to stretch the molecular chain at the start of crystallization for every molecule decreases its entropy and, thus, creates a free enthalpy barrier, hindering crystal growth even after the primary nucleation step of the crystal. As a result, a polymer melt or solution supercools in the presence of primary nuclei, even if rough surfaces obviate the need for secondary nucleation [2]. To distinguish the observed supercooling of polymer molecules in the presence of primary nuclei, this barrier to crystallization was given the name 'molecular nucleation' [1,2].

To study the details of molecular nucleation, *n*-paraffins were chosen as simple models for polyethylene. Unexpectedly, these *n*-paraffins showed no supercooling on crystallization from the melt [3]. In a detailed recent study of the heterogeneous and homogeneous nucleation of *n*-alkanes by Sirota and co-workers [4,5] and Sirota [6], similar results were reported for *n*-paraffins with $21 \leq n \leq 37$ carbon atoms. On substrates, such as microscope slides, melting point capillaries, and aluminum pans as used for differential scanning calorimetry (DSC), no additional heterogeneous nuclei are needed for crystallization, although typical dispersions of small droplets in inert liquids allows the study of supercooling caused by homogeneous nucleation. It is of the order of magnitude of 15 K for typical paraffins and 50 K for polyethylene (PE), and 70–140 K for most other polymers analyzed [2].

Questions which arise from these surprising observations are: what is the crystallization behavior of the oligomers with increasing chain lengths or what is the crystallization behavior of polymers with decreasing chain lengths other then paraffins and PE? What is the limit of chain length where a polymer behaves like a small molecule on crystallization, or how long must a molecule be before a noticeable nucleation barrier exists for crystallization?

Paraffins up to pentacontane ($C_{50}H_{102}$) and oligomer fractions of PE were analyzed earlier in a first step of this project [7–9]. These results provide a base for the discussion of the new samples. Some data were available from earlier studies of the occurrence of a small amount of reversible melting of poly(oxyethylene) (POE) and three of its oligomers [10–12]. Finally, one data-point was reported for an oligomer of poly(oxytetramethylene) (POTM) taken as reference material in a study of nanophase-separated poly(oligoamide-*alt*-oligoethers) [13,14]. The present research involved additional oligomers of POE and POTM, as well as hexacontane, $C_{60}H_{122}$. The tools to identify the reversibility are standard differential scanning calorimetry (DSC) and temperature-modulated DSC (TMDSC) in its quasi-isothermal mode. Both seeded and unseeded samples were analyzed, and a separation of supercooling due to primary crystal nucleation and molecular nucleation is attempted.

2. Experimental

Apparent heat capacity measurements were carried out with a Thermal Analyst 2920 MDSC from TA Instruments Inc., which is an isoperibol heat-flux twin calorimeter with modulation control at the sample-temperature sensor. Dry N_2 gas was purged through the differential scanning calorimeter with a flow rate of $20\,\mathrm{ml\,min^{-1}}$. A refrigerated cooling system (RCS; cooling capacity to 220 K) was used. The temperature of the equipment was initially calibrated in the standard DSC mode, using the onset temperatures of the melting transition peaks at a scanning rate of $10\,\mathrm{K\,min^{-1}}$ for water (273.15 K), indium (429.75 K), and tin (505.08 K). The heat-flow rate was calibrated with the heat of fusion of indium ($28.45\,\mathrm{J\,g^{-1}}$) and, if needed, improved with baseline and sapphire calibration runs. As references, the melting of indium and hexacontane ($C_{60}H_{122}$) were also measured in the quasi-isothermal mode of TMDSC with a 0.05 K modulation amplitude.

In the standard DSC mode, the onset melting temperature of indium, a secondary temperature standard, was set to its value of 429.75 K at $10\,\mathrm{K\,min^{-1}}$. It was found then, that a quasi-isothermal TMDSC experiment led to a melting temperature of 429.31 K. To correct the sample temperatures of the quasi-isothermal measurements, we added the difference of 0.40 K as a calibration constant to the average temperatures of the quasi-isothermal measurements at T_o. The change of the onset temperature of melting with the rate of heating is approximately 0.03 K per $\mathrm{K\,min^{-1}}$, which can account for most of this temperature difference.

The standard DSC traces were run with heating and cooling rates of 10 K min^{-1}. Both pure and mixed samples were analyzed to get information on the total heat-flow rate and the influence of crystal seeds on crystal growth. Most quasi-isothermal TMDSC was done with a sinusoidal modulation period of 60 s, a modulation-amplitude of 0.5 K, and step-wise temperature-increments of the base temperature, T_o, of 2–5 K, depending on the changes expected in the sample response. The last 10 min of the 20 min quasi-isothermal runs were used for data collection to calculate the apparent, reversing heat capacity C_p as follows [15]:

$$C_p = \frac{A_\Phi}{A_{T_s}\omega} K' \quad (1)$$

where A_Φ is the amplitude of the heat-flow rate and A_{T_s} is the amplitude of the temperature modulation. Both amplitudes are calculated as the first harmonics of the Fourier series describing the heat-flow rate and the sample temperature. The frequency in rad s^{-1} is given by ω, and K' represents the calibration constant at the given conditions of measurement. The crystallinity of the samples was determined from the heat of fusion measured by standard DSC on heating at 10 K min^{-1} prior to and after the quasi-isothermal measurements.

The new low molar mass poly(oxyethylene) fractions (POE1960 and POE3060) were purchased from Fluka. Their weight average molar masses are 1960 and 3060 Da, and their polydispersity is 1.03. The oligo(oxytetramethylene)s with number average molar masses of 650, 1000, 2000, and 2900 Da (POTM650, POTM1000, POTM2000, and POTM2900), and 98% pure hexacontane ($C_{60}H_{122}$) were purchased from Aldrich. All samples discussed in this paper are compared in Table 1. Samples of 1.5–2.5 mg were weighed on a Cahn C-33 electro-balance to an accuracy of ±0.001 mg and encapsulated in standard aluminum pans (≈23 mg, including a cover). A somewhat lighter reference pan of ≈22 mg was used for all measurements to correct easily for the asymmetry of the calorimeter by adding the reversing heat capacity from Eq. (1) for a run with an empty sample pan and the lighter reference pan to the results from the sample and reference runs (sapphire), as was described in detail in an earlier publication [16].

Table 1
Number of backbone atoms, molar masses, and chain lengths of the discussed paraffin, polyethylene fractions, oligo(oxyethylene)s, poly(oxyethylene)s, and oligo(oxytetramethylene)s

Samples	Number of backbone atoms	Molar mass (Da)	Chain length[a] (nm)
$C_{60}H_{120}$	60	844	7.46
PE560[b]	40	560	5.09
PE1150[b]	82	1,150	10.4
PE2150[b]	153	2,150	19.2
POE1000[c]	68	1,000	6.26
POE1500[d]	102	1,500	9.39
POE1960	133	1,960	12.2
POE3060	208	3,060	19.2
POE5000[d]	310	4,560	28.5
POE35000[d]	2,380	35,000	219
POE300000[c]	20,430	300,000	1880
POTM650	45	650	5.44
POTM1000	69	1,000	8.37
POTM2000[e]	139	2,000	16.7
POTM2900	201	2,900	24.3

[a] In the orthorhombic structures for $C_{60}H_{122}$ and PE, the monoclinic POE structures, with $c = 1.93$ nm (3*7/2 helix), and the moniclinic POTM structures with $c = 1.207$ nm for POTM, (5*2/1 helix) [2].
[b] Research reported in [9].
[c] Research reported in [12].
[d] Research reported in [10,11].
[e] Research reported in [13,14].

3. Results and preliminary discussion

The various, newly measured samples are described in order of molar mass and compared to the previous data. The literature consists of data for paraffins and polyethylene [7–9], POE1000 [12], POE1500 [10], POE5000 and POE35000 [11], POE300000 [12], and a single sample of POTM2000 [13,14]. An final discussion of the results and conclusions are given in Section 4.

3.1. Paraffins and polyethylene fractions

Hexacontane is a new paraffin analyzed in this research. It serves as a reference of oligomer crystals in equilibrium, and extends the analyzed paraffins which melt reversibly from $C_{50}H_{102}$ to $C_{60}H_{122}$. The discussion also summarizes the earlier work published on the reversing melting of paraffins, PE, and low molar mass fractions of PE [3–9]. Note that the term

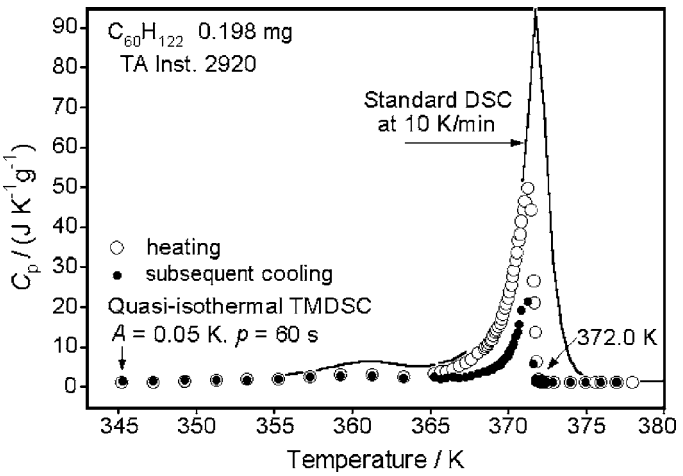

Fig. 1. Apparent specific heat capacities measured by standard DSC and quasi-isothermal TMDSC with hexacontane, using a small temperature modulation of 0.05 K.

"reversing" is used when describing data derived from Eq. (1) which may still contain time-dependent, irreversible effects as well as analysis flaws due to lack of steady state and stationarity. The term "reversible" is reserved to its thermodynamic meaning. One must remember, however, that slow processes may lose their reversibility when the applied analysis rate outruns the response of the sample and the temperature is changed before the process to be studied has reached equilibrium.

3.1.1. Hexacontane

Fig. 1 shows a standard DSC trace on heating for $C_{60}H_{122}$ and a set of quasi-isothermal TMDSC runs on first heating of the sample as delivered, followed by step-wise cooling after reaching the melt. The main melting peaks by DSC and TMDSC follow the same contour up to about 60% of the peak height. Beyond this point, the standard DSC shows an increasing instrument lag [17]. Similarly, the TMDSC with its small modulation amplitude cannot complete the melting and crystallization required for reaching full equilibrium within each cycle, as was shown in detail earlier [7,8]. The TMDSC peak-width of reversible melting is about 1.0 K. The peak narrows on cooling, an indication of better crystallization on the slower cooling with modulation. The shallow premelting peak at about 361 K is much smaller in TMDSC, evidence of the presence of some irreversibly melting material.

The results in Fig. 1 are similar to those by the earlier studies on paraffins which included data up to $C_{50}H_{102}$ [4–9]. The melting temperature and width of the peak depends on the purity of the sample and the quality of the crystals. The narrowest peaks of our samples were found for $C_{26}H_{54}$ and $C_{50}H_{102}$. For these, 0.1 K covered more than 60% of the overall melting [8]. The melting of the paraffins up to $C_{60}H_{122}$ is, thus, largely reversible, and for purer and better crystals, it may be fully reversible.

The paraffins were earlier linked to the oligomers PE560 and PE1150, fractions of polyethylene of narrow molar mass distribution [9]. The PE560 with an average of 40 backbone atoms has a melting peak that covers more than 30 K and indicates a multi-component, eutectic phase diagram. The quasi-isothermal TMDSC endotherm reached about half the standard DSC peak height (6.0 J K g^{-1}), an indication of at least partially reversible melting. Furthermore, the TMDSC indicated also no supercooling on crystallization. The PE1150 with an average of 82 backbone atoms still has a broad melting peak, although the main peak is narrower and higher than that of PE560. The apparent reversing specific heat capacity reached to only about 10% of the standard DSC peak height (2.5–6.0 J K g^{-1}, depending on crystallization history) and shows a supercooling of 4.1 K. These data suggest that for paraffins and oligomers of polyethylene the critical chain-length for reversible

crystallization under the given crystallization conditions is about 75 backbone-chain atoms which is equivalent to a crystal thickness of about 10 nm.

The POE1000 [12] shows also a very broad melting peak, but a much smaller reversing melting peak than PE1150 which, in addition, exists only for poorly crystallized samples, so that practically all melting is irreversible. The crystallization temperature can be gained from the limited data to be between 305 and 308 K. The attainment of the heat capacity of the liquid after melting is not clearly seen, but is close to the equilibrium melting temperature of 313.0 K, calculated from Eq. (2), later. The POE1500, first analyzed in [11], and studied in detail in [10], also shows a small reversing melting peak for fast crystallized samples, and none for slowly crystallized samples. The supercooling can be read from the quasi-isothermal TMDSC plots and Lissajous figures to be a maximum of 8.0 K and a minimum 2.0 K, respectively. On slow crystallization, all samples discussed in this Section are expected to reach the extended chain macroconformation.

3.2. Poly(oxyethylenes) and its oligomers

The crystal structure, melting and crystallization kinetics of the polyoxyethylenes are well known. In the crystal, the backbone chain assumes a helix of type 3*7/2 [2]. The equilibrium melting temperatures have been derived from extensive experiments on POE fractions as [18–20]

$$T_m^o = 340.8 - \frac{1890}{x} \quad (2)$$

where x represents the number of backbone chain atoms.

3.2.1. POE1960

Fig. 2 represents the standard DSC, and quasi-isothermal TMDSC results for the heating of POE1960. The peak temperature by standard DSC is 326.6 K, close to the equilibrium melting temperature calculated from Eq. (2). The crystallinity from the standard DSC run is 62%. The apparent reversing heat capacity shows only a very small contribution to melting.

Fig. 3 displays an enlarged plot of the apparent, reversing heat capacity of POE1960. The dotted line is the baseline heat capacity of the liquid amorphous sample, as given in the *ATHAS* Data Bank [21,22]. The solid line is computed from the Data Bank values for the crystalline and amorphous states of POE in a 62% crystalline sample. The end of melting on heating occurs at 324.9 K, and the beginning of crystallization on cooling is seen at 319.6 K. The difference of about 5.3 K represents the experimental supercooling of POE1960. From the equilibrium melting temperature of 326.2 K of Eq. (2), the supercooling is 6.6 K. On cooling, the POE1960 does not develop a reversing melting peak. Its apparent, reversing heat

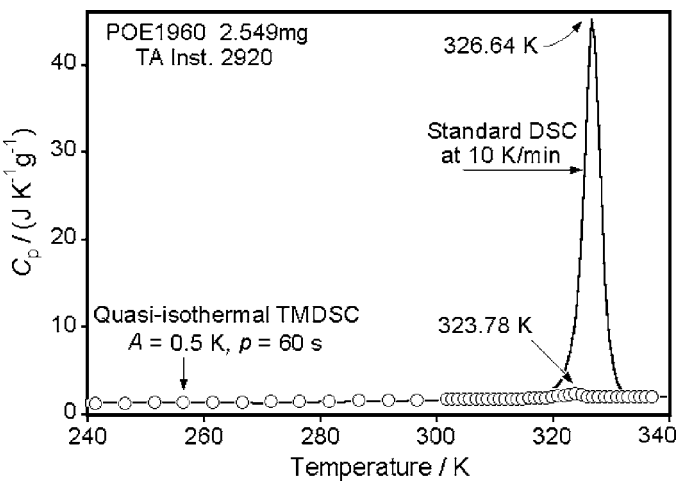

Fig. 2. Apparent specific heat capacities measured by standard DSC and quasi-isothermal TMDSC for POE1960, using a modulation of 0.5 K.

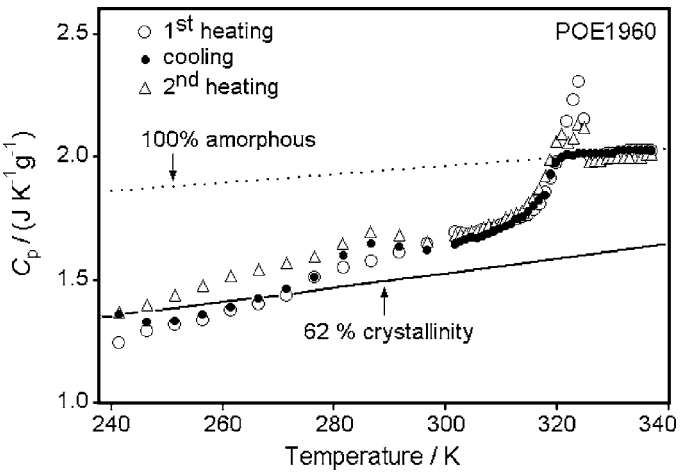

Fig. 3. Enlarged plots of the apparent, reversing specific heat capacities of POE1960 on stepwise heating and cooling, measured by quasi-isothermal TMDSC. The first heating run is identical to the one depicted in Fig. 2.

capacity matches the crystals at a level close to that of the melt. The second heating runs exhibit that the end of melting is at same temperature as the first heating run, and the small maximum is lower than on first heating. A second cooling run for POE1960 is identical to the first and not depicted in Fig. 3.

Below room temperature, the apparent, reversing plot of C_p on cooling and heating is the same within experimental error. (The error is somewhat higher in the low-temperature region because of cooling problems during this particular measurement.) The glass transition is located at 206 K and not shown in Fig. 3. Since major melting starts only at 320 K (see Fig. 2), the excess heat capacity between 240 and 320 K is likely to be caused only by conformational contributions, as could be proven to be the case for polyethylene [23]. A crystalline α-transitions in dynamic mechanical measurements, was seen for PE, POE, and POTM, is usually assigned to conformational motion in the crystal [12], and all three show a similar excess heat capacities in their crystals.

The polyethylene fraction PE2150 has similar average molar mass and was analyzed in the same fashion as the POE samples in this research [9]. The PE2150 has a considerably higher reversing peak height than POE1960 in Fig. 3 (1.8 and 1.0 J K^{-1} g^{-1} for the first and second heatings, respectively), but less than for the oligomer PE1150, mentioned previously. We speculate that the lower limits of these melting peaks which are seen on the second heating (after slow crystallization) are a measure of reversible melting of lower mass species, while the additional reversing melting on first heating, seen in both PE and POE samples, is caused by nonequilibrium crystallization, as was suggested in the extensive analysis of POE1500 [10].

3.2.2. POE3060

Fig. 4 displays the apparent specific heat capacity for POE3060 in the same fashion as the POE1960 data are given in Fig. 2. Two endothermic peaks are in the standard DSC trace, a small one at 325.9 K and the major melting peak at 331.8 K. The first peak does not show in the reversing data and agrees with the melting of once-folded chains [10]. On cooling at 10 K min^{-1}, the low-temperature peak disappears almost completely in the standard DSC trace [3]. The major melting peak is located at the equilibrium melting temperature, given by Eq. (2). Overall, the major melting peak is somewhat sharper and narrower than the melting peak of POE1960, as one would expect for a fraction of higher mass, since the components should have less of a lowering of the melting temperature for a similar polydispersity. The apparent, reversing C_p has only a barely visible peak at 328.9 K.

Fig. 5 shows the enlarged and augmented TMDSC traces. As in Fig. 3, there is little excess C_p beyond the expected contribution from the conformational heat capacity. The reversing peaks are small and decrease

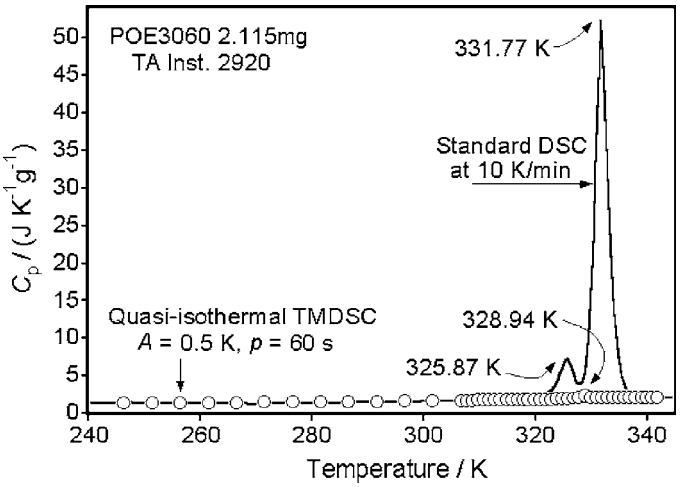

Fig. 4. Apparent specific heat capacities measured by standard DSC and quasi-isothermal TMDSC for POE3060, using a modulation of 0.5 K.

further on better crystallization. The onset of crystallization on cooling is at 318.7 K, a supercooling of about 13 K from the melting of the extended chain crystals, and about 7 K from the once-folded crystal. It is more likely that once-folded or non-integral crystals grow first and anneal subsequently before melting to the extended-chain macroconformation [2].

The POE5000 which has an only 60% larger molar mass than POE3060 was analyzed earlier [11]. Its end of melting by TMDSC was found at 333.7, still close to the equilibrium of Eq. (2). The crystallization on quasi-isothermal TMDSC on cooling occurred at 313.7, a supercooling of 20 K, which would be reduced considerably by assuming the first growing crystals consist of less perfect crystals. The melt-end by quasi-isothermal TMDSC for POE35000 [11] and POE300000 [12] were seen at about 338 K, about 3 K below their equilibrium melting temperature, a lowering caused mainly by chain folding. The crystallization by quasi-isothermal TMDSC on cooling was seen

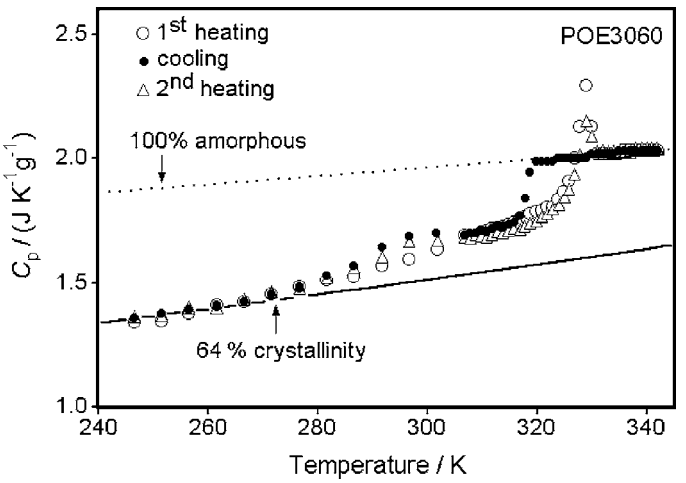

Fig. 5. Enlarged plots of the apparent, reversing specific heat capacities of POE3060 on stepwise heating and cooling, measured by quasi-isothermal TMDSC. The first heating run is identical to the one depicted in Fig. 4.

at about 323 K, a supercooling of about 15 K. Both these polymers have sizeable reversing peaks on heating (0.4–0.6 $J\,K^{-1}\,g^{-1}$, depending on the quality of the crystals [12], compare to Figs. 1, 3, and 5). On cooling, the heating curve is almost reached, but because of the large supercooling, much of the peak is avoided, still, the reversing heat capacity is larger than that of the melt. Polyethylenes of higher molar mass have also been analyzed [9]. In this case, the reversing melting peak on heating is much larger (broader and also somewhat higher, $\approx 0.7\,J\,K^{-1}\,g^{-1}$) and remains sizeable on cooling ($0.3\,J\,K^{-1}\,g^{-1}$). The supercooling is less, only about 5.5 K.

3.3. Oligo(oxytetramethylene)

Poly(oxytetramethylene) is the first member of the homologous series of polyoxides that does not have a helical chain structure. The packing in the chains in the crystals is related to the monoclinic structure of PE with maximum interaction of the oxygen dipoles [2]. Fig. 6 illustrates standard DSC heating traces of the as-received samples followed by the cooling traces of all POTM samples analyzed. The POTM650 has an average of 45 backbone atoms. It possesses a broad melting range with three shallow peaks of increasing heights, marked I, II, and III, but only one reasonably sharp crystallization peak. The POTM1000 has two melting peaks on heating (I and II), but also only one on cooling. The width of the melting transitions is narrower than seen for POTM650. Finally the POTM2000 and POTM2900 melt more sharply and crystallize with melting peaks similar in width to the samples of lower molar mass. The reasons behind the changing broadening of the melting range and appearance of multiple melting peaks are typical for eutectic phase diagrams for solutions of lower mass, and also annealing to longer fold-lengths after initial crystallization. Only a preliminary degree of supercooling can be estimated from these standard DSC traces by taking the differences of onset temperatures. In case the initially grown crystals on cooling correspond to the lower melting peaks seen on heating, POTM650 would show no, and POTM1000 about 11 K of supercooling. The two oligomers of higher mass, POTM2000 and POTM2900, have 15–20 K supercooling. Refinements from the quasi-isothermal experiments and seeded crystallization are described next.

3.3.1. POTM650

It is difficult from Fig. 6 to say precisely where POTM560 starts to crystallize on cooling and what is the corresponding melting peak. For this reason, the standard DSC experiment was repeated with more details, as shown in Fig. 7. The analysis was started with cooling from the melt (DSC trace 1), followed by

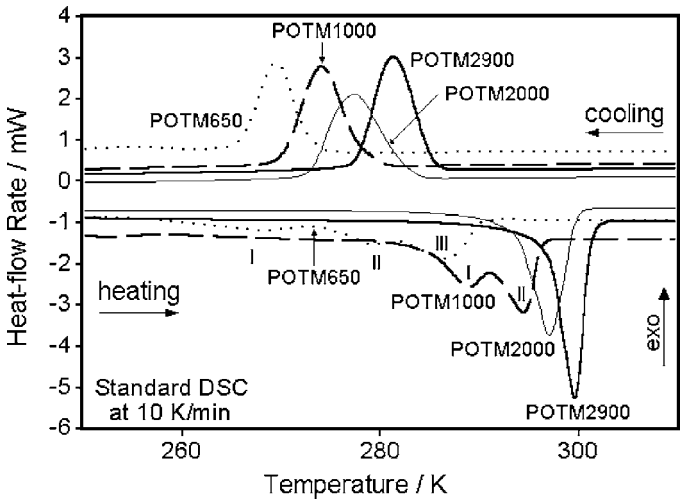

Fig. 6. Standard DSC heat-flow-rate data for the POTM oligomers of Table 1 as a function of temperature on heating, followed by cooling. Multiple melting peaks are labeled I, II, and III.

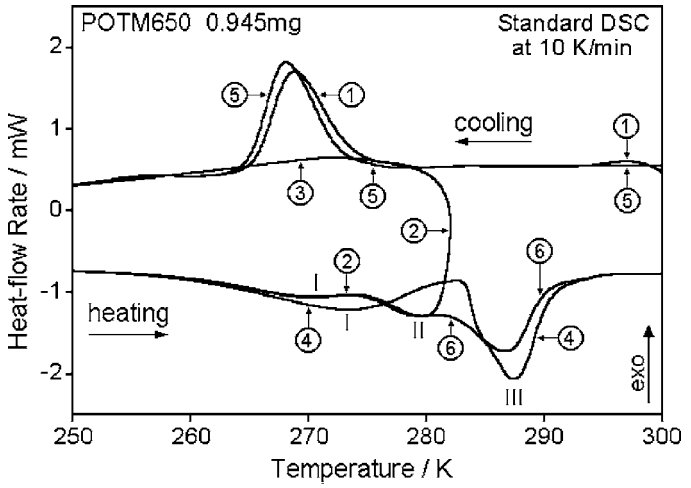

Fig. 7. Standard DSC heat-flow-rate data for POTM650 as a function of temperature on several cooling and heating cycles. Multiple melting peaks are labeled I, II, III, and the sequence of cooling and heating is indicated by the numbers 1–6.

heating up to the melting peak II (trace 2) and cooling for renewed crystallization in the presence of the crystals of melting peak III (trace 3). Next, the experiment was continued by reheating to the melt (trace 4), renewed crystallization on cooling without any nuclei (trace 5) and, for reference, a final heating (trace 6). All cooling traces show a very gradual start of crystallization, with trace 3 missing the main crystallization peak shown in traces 1 and 5. The melting trace 4 indicates a missing peak II and perfected peaks I and III. These results must mean that peaks I represent the eutectic melting with different degrees of perfection. peak II represents the melting of metastable crystals, which under better crystallization conditions perfect and melt within the peaks I and III, both shifted to somewhat higher temperatures, and peak III represents the pure large chain-length components.

The quasi-isothermal TMDSC traces for POTM650 run parallel to the DSC traces 5 and 6 and are displayed in Fig. 8. The three melting peaks correspond

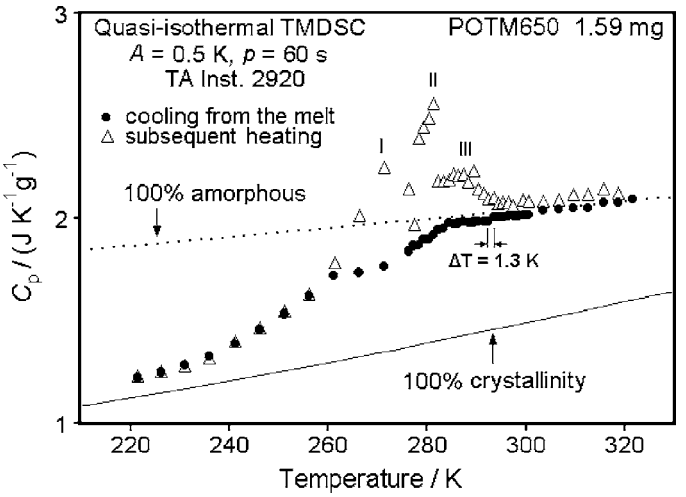

Fig. 8. Apparent specific heat capacities measured by quasi-isothermal TMDSC for POTM650 on cooling and subsequent heating.

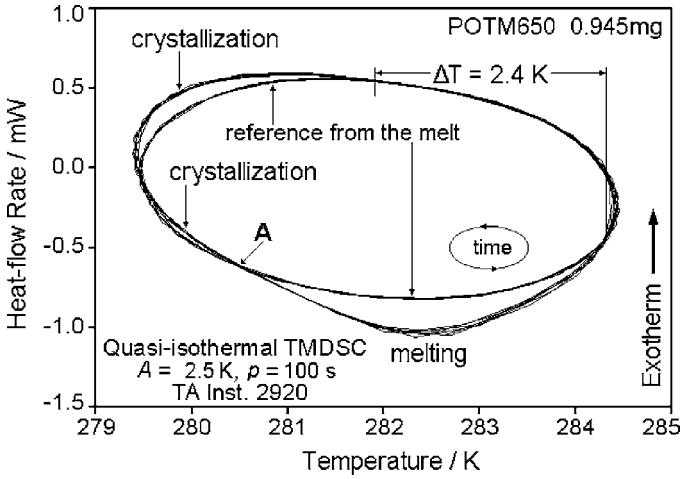

Fig. 9. Lissajous figure of a quasi-isothermal TMDSC run covering melting and crystallization. The perfect ellipse is superimposed from a measurement in the melt.

to Figs. 6 and 7 at about 270 K (I), 280 K (II), and 287 K (III). The end of melting on heating occurs at 297.5 K. On cooling of POTM650, there is no excess apparent reversing heat capacity beyond that of the melt. A minor drop in the reversing heat capacity occurs approximately at the end of peak III. A larger drop begins at the melting peak II, and starting from 260 K, the C_p on cooling agrees with the C_p on heating.

Further details can be seen in Fig. 9, where a Lissajous figure, a plot of the heat-flow rate versus the temperature, is reproduced for modulation about a small portion of the heating and cooling traces 2 and 3 of Fig. 7. The modulation had an amplitude of 2.5 K and a period of 100 s, so that both crystallization and melting could just be reached in one modulation cycle. We expect the experiment to cover the upper region of the eutectic melting peak I in Fig. 7. The melting peak II should have been shifted into III, as indicated by trace 4. Fig. 9 shows a number of cycles after a steady state had been reached. For the interpretation of the deviation from an ellipse without melting and crystallization, an identical reference cycle from the melt is superimposed. The difference, ΔT, from the end of melting to the beginning of crystallization is 2.4 K, with crystallization beginning close to T_o, the mid-temperature of modulation. This ΔT is, however, only an upper limit, since it contains the assumption that there is no reorganization during the 65 s between the first crystallization and the last melting. The sharp cross-over at point A suggests that melting and crystallization might overlap from A to T_o. Assuming that the marked step in Fig. 8 indicates the supercooling of the crystals that melt under peak III, gives a value of 1.3 K. Unique for POTM is the very slow rate of crystal growth in both, the high temperature region in Fig. 8 (melting at peak III) and the low temperature region in Fig. 9 (melting at peak I).

3.3.2. POTM1000

Fig. 10 represents the results for POTM1000. The crystallinity determined from the heat of fusion measured by standard DSC is 46%. In the standard DSC trace of Fig. 6, there are two melting peaks (I and II), of which peak I is dependent on the thermal history. In the apparent, reversing C_p trace of Fig. 10, there is no peak I, only a small peak II can be seen, as marked. On second heating, the better crystallized sample shows almost no peak II. Again, it is difficult to say where the crystallization starts on cooling because the reversing heat capacity of the liquid contained larger deviations. The reversing heat capacities on cooling gradually drop below the liquid heat capacity from around 287 K and then reach the value of 56% semicrystalline heat capacity at about 220 K. The end of melting on first heating occurs at 299 K. The onset of crystallization on first cooling is approximately 297.3 K, suggesting a supercooling of 11 K. A multiple cooling and heating run, as seen for POTM650 in

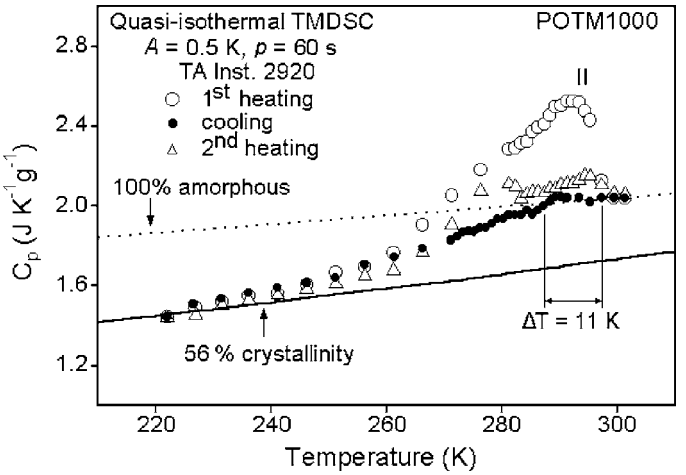

Fig. 10. Plots of the apparent, reversing specific heat capacities of POTM1000 on stepwise heating and cooling, measured by quasi-isothermal TMDSC.

Fig. 7, indicates also considerable reorganization for POTM1000 and a very small supercooling on crystallization in the presence of remaining crystals, so that the minimal supercooling may be as little as 2 K.

3.3.3. POTM2000

Fig. 11 exhibits the quasi-isothermal TMDSC traces of POTM2000. There are two minor reversing melting peaks on first and second heating. The low temperature peak does not show in the standard DSC of Fig. 6, but can be seen as a small shoulder when enlarged as shown in reference [14]. The high temperature peaks are located at about 300 K on both DSC and TMDSC traces, and the end of melting on both TMDSC heating runs occur at 305.5 K. The beginning of the crystallization from the melt in both, Figs. 6 and 11, occur at about 286 K, yielding an about 20 K supercooling. Repeating the experiment of Fig. 7 for POTM2000, one finds that cooling after incomplete melting moves the crystallization peak to about 10 K

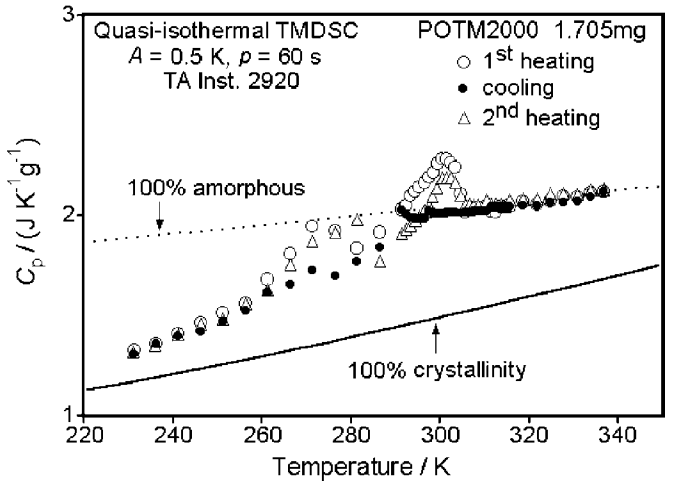

Fig. 11. Plots of the apparent, reversing specific heat capacities of POTM2000 on stepwise heating and cooling, measured by quasi-isothermal TMDSC.

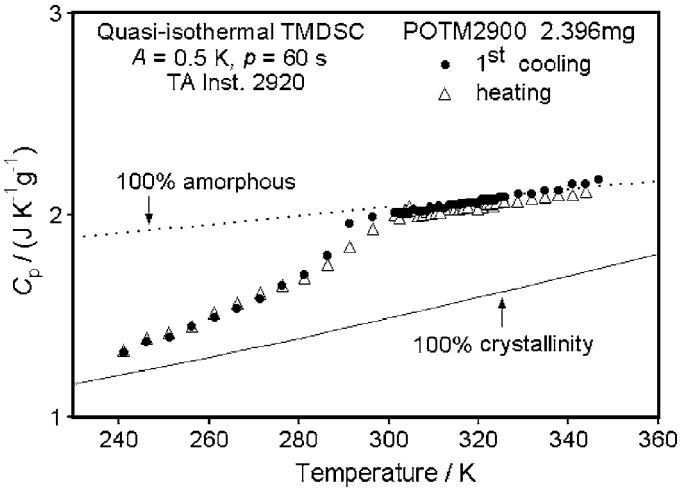

Fig. 12. Plots of the apparent, reversing specific heat capacities of POTM2900 on stepwise heating and cooling, measured by quasi-isothermal TMDSC.

supercooling without showing the rather low rates of crystallization seen in curve 3 of Fig. 7 for POTM650.

3.3.4. POTM2900

Fig. 12 represents the quasi-isothermal TMDSC traces of POTM2900. There is hardly any apparent reversing heat capacity contribution due to melting on heating and due to crystallization on cooling. From a recording of the modulated heat-flow rate versus time, the beginning of crystallization is determined to be 296.4 K, and the end of melting, to be 307.6 K. The difference of about 11 K is taken as the degree of supercooling of POTM2900. Fig. 13 shows standard DSC traces as in Fig. 6, but starting at room temperature with a sample annealed for a long time at this temperature. Its melting shows an additional high-temperature peak which is most likely the melting of the extended-chain conformation. Its end of melting occurs at about 15 K higher than the melting in Fig. 6 and increases the supercooling to over 30 K.

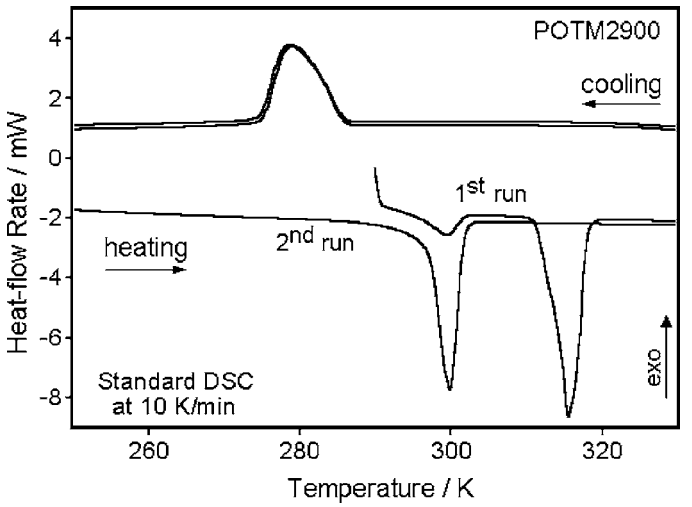

Fig. 13. Standard DSC heat-flow-rate data for POTM2900 as a function of temperature on heating and cooling.

4. Final discussion and conclusions

These DSC and TMDSC experiments on paraffins and oligomers of poly(oxyethylene)s and poly(oxytetramethylene)s show several important properties:

1. All analyzed samples, as well as the discussed literature data, show an excess of reversible heat capacity over the computed level based on the vibrational spectrum [24]. For crystals of polyethylene and the paraffins this excess heat capacity originates from conformational contributions which also are the cause for the α-relaxation observed by dynamic mechanical analysis [25]. Poly(oxyethylene) and poly(oxytetramethylene) show similar relaxations, and all three polymers are known to perfect on annealing by thickening of the crystals involving sliding diffusion [12].
2. Reversible melting and crystallization are found for the paraffin $C_{60}H_{122}$. All other analyzed oligomers melt largely irreversibly, although the POTM650 may show a small amount of fully reversible melting, but much less than seen in the equivalent PE560 [9]. The reversing melting peaks seen in Figs. 3, 5, 8, and 10-12 are rather small, and decrease with crystal perfection. Both, POTM2900 of this research and the POE5000 of reference [11], melt fully irreversibly. At larger molar mass, as for POE35000 [11] and POE300000 [12], PE15200 [9] and PE130000 [9,26], the reversing melting increases again, most likely due to incomplete melting of polymer molecules during the modulation cycle.
3. All polymer fractions show signs of annealing which starts immediately after the crystallization and lead to multiple melting peaks (see Figs. 6, 7, and 13). In some cases, this annealing goes in recognizable steps of reduction of the number of chain folds [20]. The polymer fraction POTM650 has, in addition, a broadened melting range towards lower temperature due to segregation into different eutectic fractions, as also seen in PE560 [11].
4. In Fig. 14, the supercooling of the newly measured samples is compared to the earlier available data on paraffins and polyethylenes [3,8,9]. The paraffins and the low-molar-mass fractions were independent of primary nucleation, while the higher-molar mass polyethylenes were seeded to exclude primary nucleation effects. These data showed clearly that there is a critical length in backbone atoms above which molecular nucleation starts to be important for the description of the crystal growth. The critical length is about 75 backbone atoms, or about 10 nm of extended-chain length of the crystals, far below the critical length of chain folding which is observed for polyethylene for chain lengths longer than 37 nm [27,28].
5. The lower values of supercooling for the newly measured oligooxides listed in Fig. 14 correspond to reversing melting thought to have occurred

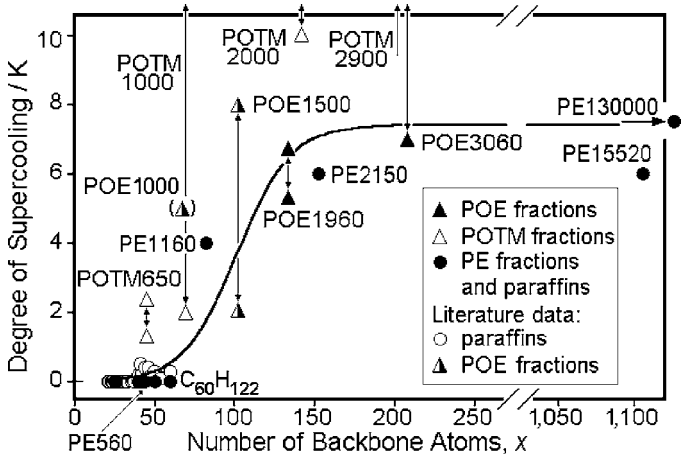

Fig. 14. Degree of supercooling as a function of the number of chain atoms in the backbone of the materials listed in Table 1 and additional paraffins [8] and polyethylene fractions and whole polymers [9].

with a minimum of reorganization and most likely without the need of primary nucleation. These data seem to parallel the drawn-out curve derived for the CH_2-based molecules, i.e. they also have a critical molar mass of about 75 backbone atoms for major supercooling due to molecular nucleation, although the minimum seems not reach zero supercooling, i.e. there may not be a fully reversible melting until shorter lengths than 45 chain atoms are reached. The upper points marked in Fig. 14 are most likely set by the need of primary nucleation and lead to much larger supercoolings for the polyoxides. For the polyethylene, this supercooling is about 10 K. The higher molar mass oligomers of POE and POTM, in contrast, reach values as high as 30 K. This supercooling due to primary nucleation marked by the upper points decreases also with decreasing molar mass at similar chain length.

Thermal analysis with DSC and TMDSC allows a much deeper insight in the various processes involved in crystallization and melting. For well-crystallized samples, the low molar mass examples cover the range from fully reversible melting, as in $C_{60}H_{122}$ (Fig. 1), to fully irreversible melting as in POE5000 (11) and POTM2900 (Fig. 12). As soon as the molar mass reaches that of a polymer (>10,000 Da) reversing contributions arise again. The reversing contributions in samples of low molar mass distributions may be due to diffusion-based reorganization into more stable crystal-size distributions [10]. In samples of high molar mass, they may be due to partial melting which on cooling, can avoid molecular nucleation and set up local melting equilibria [11].

Acknowledgements

This work was supported by the Division of Materials Research, National Science Foundation, Polymers Program, Grant no. DMR-9703692 and the Division of Materials Sciences, Office of Basic Energy Sciences, US Department of Energy at Oak Ridge National Laboratory, managed and operated by UT-Battelle, LLC, for the US Department of Energy, under contract number DOE-AC05-00OR22725.

References

[1] B. Wunderlich, Disc. Faraday Soc. 68 (1979) 239.
[2] B. Wunderlich, Macromolecular Physics, vols. 1–3, Academic Press, New York, 1974, 1976, 1980.
[3] J. Pak, Master and Ph.D. Theses, Deptartment of Chemistry, The University of Tennessee, Knoxville, TN, USA, 2000, 2001.
[4] H. Kraack, E.B. Sirota, M. Deutsch, J. Chem. Phys. 112 (2000) 6873.
[5] H. Kraack, M. Deutsch, E.B. Sirota, Macromolecules 33 (2000) 6174.
[6] E.B. Sirota, Langmuir 13 (1998) 3133.
[7] J. Pak, A. Boller, I. Moon, M. Pyda, B. Wunderlich, Thermochim. Acta 357–358 (2000) 259.
[8] J. Pak, B. Wunderlich, J. Polym. Sci., Part B: Polym. Phys. 38 (2000) 2810.
[9] J. Pak, B. Wunderlich, Macromolecules 34 (2001) 4492.
[10] K. Ishikiriyama, B. Wunderlich, J. Polymer Sci., Part B: Polym. Phys. 35 (1997) 1877.
[11] K. Ishikiriyama, B. Wunderlich, Macromolecules 30 (1997) 4126.
[12] W. Hu, T. Albrecht, G. Strobl, Macromolecules 32 (1999) 7548.
[13] M.L. Di Lorenzo, M. Pyda, B. Wunderlich, J. Polym. Sci., Part B: Polym. Phys. 39 (2001) 1594.
[14] M.L. Di Lorenzo, M. Pyda, B. Wunderlich, J. Polym. Sci., Part B: Polym. Phys. 39 (2001) 2969.
[15] B. Wunderlich, Y. Jin, A. Boller, A. Thermochim. Acta 238 (1994) 277.
[16] K. Ishikiriyama, B. Wunderlich, J. Thermal Anal. 50 (1997) 337.
[17] A. Boller, M. Ribeiro, B. Wunderlich, J. Thermal Anal. Cal. 54 (1998) 545.
[18] C.P. Buckley, A.J. Kovacs, Prog. Coll. Polym. Sci. 58 (1975) 44.
[19] C.P. Buckley, A.J. Kovacs, Coll. Z. Z. Polym. 254 (1976) 695.
[20] S.Z.D. Cheng, B. Wunderlich, J. Polym. Sci., Part B: Polym. Phys. 24 (1986) 577.
[21] U. Gaur, H.-C. Shu, A. Mehta, S.-F. Lau, B.B. Wunderlich, M. Varma-Nair, B. Wunderlich, J. Phys. Chem. Ref. Data 10 (1981) 89, 119, 1001, 1051; 11 (1982) 313, 1065; 12 (1983) 29, 65, 91; 20 (1990) 349. For easy access, use the internet home page of the *ATHAS* laboratory: web.utk.edu/~athas
[22] J. Grebowicz, B. Wunderlich, Polymer 26 (1985) 561.
[23] B.G. Sumpter, D.W. Noid, G.L. Liang, B. Wunderlich, Adv. Polym. Sci. 116 (1994) 27.
[24] J. Grebowicz, H. Suzuki, B. Wunderlich, Polymer 26 (1985) 561.
[25] B. Wunderlich, The Basis of Thermal Analysis, in: E. Turi (Ed.), Thermal Characterization of Polymeric Materials, 2nd ed., Academic Press, New York, 1997, p 389.
[26] B. Wunderlich, C.M. Cormier, J. Phys. Chem. 70 (1966) 1844.
[27] D.C. Bassett, R.H. Olley, S.J. Sutton, A.S. Vaughan, Macromolecules 29 (1996) 1852.
[28] D.C. Bassett, R.H. Olley, S.J. Sutton, A.S. Vaughan, Polymer 37 (1996) 4993.